FACILITY FORM 602

N66-15273
(ACCESSION NUMBER)

40
(PAGES)

CR 69846
(NASA CR OR TMX OR AD NUMBER)

(THRU)

1
(CODE)

33
(CATEGORY)

STEADY STATE AEROTHERMOCHEMISTRY FOR LIQUID BIPROPELLANT ROCKET MOTORS

GPO PRICE $ ______

CFSTI PRICE(S) $ ______

Hard copy (HC) 2.00

Microfiche (MF) .50

ff 653 July 65

Prepared For

Jet Propulsion Laboratory
Pasadena, California
under NAS 7-100

Report No. 64.3
1 October 1964

Vito D. Agosta
Vito D. Agosta
Consultant

VITO D. AGOSTA

STEADY STATE AEROTHERMOCHEMISTRY FOR LIQUID BIPROPELLANT ROCKET MOTORS

V. D. Agosta

S. Z. Burstein

Prepared For

Jet Propulsion Laboratory
Pasadena, California

Report No. 64.3
1 October 1964

Vito D Agosta

Vito D. Agosta
Consultant

CONTENTS

STEADY STATE AEROTHERMOCHEMISTRY FOR LIQUID BIPROPELLANT ROCKET MOTORS

by

V. D. Agosta and S. Z. Burstein

ABSTRACT

15273

A model is proposed for the combustion of a bipropellant spray in a rocket motor. The model includes three subsystems: the fuel droplets, the oxidant droplets, and the combustion gases. The fuel droplet ballistics are determined by assuming a diffusion controlled evaporating droplet; thus it follows that fuel vaporization serves as the rate-controlling combustion process. A Knudsen-Langmuir kinetic model is assumed for the evaporation of the oxidant droplets. The combustion gases are generated by the combustion of the evaporated propellants at the local O/F ratio. The solution to this problem requires solving the coupled equations for heat, mass and momentum transfer for the fuel and oxidant droplets and vapors, and combustion gases, and also the chemical equilibrium equations for varying oxidant-fuel ratio. One-dimensional compressible gas dynamics is assumed. The results of this analysis give the mass distribution of oxidant and fuel vaporization, and subsequent combustion, along the axis of the rocket motor.

Author

NOMENCLATURE

A	area
C_D	drag coefficient
C_ℓ	specific heat of liquid
C_p	specific heat at constant pressure
D_v	diffusion coefficient
E, e	internal energy
F, f	frictional force on droplets
G	mass
g	gravitational constant
h	enthalpy
h_v^o	defined by Eq. (16d)
K	thermal conductivity
K_g	coefficient of mass transfer
K_m	mean film conductivity
M	molecular weight
m	mass
N	molecular or droplet number
Nu	Nusselt number
n	unit normal
Pr	Prandtl number
p	pressure
Q	heat transfer
$\overline{Q}$	heat transfer from gas

Q_L, λ	latent heat of vaporization
q	defined by Eq. (16b)
Re	Reynolds number
R_o	universal gas constant
r	droplet radius
Sc	Schmidt number
s	surface
t	time
u	gas velocity
v	droplet velocity, molecular velocity
W, w	work, mass
We	Webber number
w	liquid surface velocity
x	coordinate
y	nondimensional distance
Z	defined by Eq. (22b)
z	defined by Eq. (22a)
α	defined by Eq. (27)
δ	film thickness
μ	viscosity
ν	volume, molecular population density
ρ	density
σ	geometric standard deviation
φ	total mass of combustion gas flowing

Subscripts

c	critical state
D	diffusing vapor
d	droplet
g	gas
i,j,N	counting indices
j	droplet group
ℓ	liquid
s	surface
v, vap	vaporization
1	initial

Superscript

o	stagnation

STEADY STATE AEROTHERMOCHEMISTRY FOR LIQUID BIPROPELLANT ROCKET MOTORS

I. INTRODUCTION

In this report, the model and theoretical equations describing the liquid propellant droplet ballistics and the combustion gas behavior are given. An algorithm of the suggested solution technique is presented and the areas in which computational difficulties are expected. Possible modifications to the analysis are given to allow for injector design.

It is recognized that the aerodynamic, hydrodynamic and combustion processes occurring in a rocket motor are so complex that at this time they do not admit theoretical formulation. Thus the problem at hand is to determine and reduce these formulations consistent with a combustion spray model which retains the essential characteristics of those processes occurring in a rocket motor. The development of the model and the equations will allow, as much as possible, their inclusion to the instability analysis, their modification for injector design, and propellant evaporation relaxation. In the evaporation and combustion of a propellant spray, droplet interaction is neglected. This assumption allows for a concentrated region of droplets to occur in a chamber; however, the condition that their evaporation rates are cumulative can give a quantitative error. (Refer to the work of Toong and of Gerstein). In steady state operation, it is felt that the occurrence of the above situation is not significant.

Combustion in a rocket motor is controlled in part by the evaporation processes of an arbitrary number of fuel and oxidant droplets which have been injected into the chamber. The evaporation of these droplets is affected by their immediate environment, which is composed of hot, high velocity gases. The environment, however, is generated by these evaporating and combusting propellant droplets; thus a strong coupling exists between the aerodynamics of the gas streams, hydrodynamics of the propellant jets, evaporation of the drops, and combustion. In most propellant systems one liquid component evaporates at a significantly faster rate than the other. Thus a flame will stabilize in those regions which contain gas mixtures within the limits of flammability.

For hydrazine-nitrogen tetroxide propellant combinations, the nitrogen tetroxide has a higher vapor pressure than hydrazine; thus, in a similar aerothermodynamic environment, it will vaporize at a faster rate. One may then envisage that a flame will propagate and ultimately shroud the hydrazine droplets. The combustion model reduces to a fuel droplet surrounded by a combustion gas-hydrazine vapor mixture which in turn is shrouded by a flame, and beyond the flame a mixture of combustion gases and nitrogen tetroxide (or dissociated components) vapor. Starting with the oxidant droplet, it is then considered that it evaporates into a combustion gas-oxidant vapor mixture which mixes with the combustion gases according to Gibbs-Dalton's Law. At a point where dissociation becomes significant, e.g., 2500°R, a chemical reaction takes place between the oxidant vapor and the combustion gases. Beyond this point and proceeding along the outward radial direction, a combustion gas temperature is attained corresponding to the adiabatic flame temperature at the local O/F ratio and satisfying the requirements of thermodynamic equilibrium. This concentric spherical film around the oxidant droplet serves to define an effective heat transfer coefficient for heat transfer to the drop, and equally important, serves to determine, from kinetic theory, an equivalent accommodation coefficient. Although the whole heterogeneous field is reacting chemically, the major degree of reaction (or chemical energy liberation) occurs in the flame shroud surrounding the fuel droplet. It is seen that the above model contains both heterogeneous systems (liquid propellants and gases) and premixed systems (fuel vapor and combustion gas between droplet surface and flame). The participation of these systems into supporting combustion instability is dependent on the wave geometry and velocity (wave residence time).

As stated previously, the evaporation of propellant sprays is treated as a summation of the vaporization of individual droplets. The general reliability of droplet drag and evaporation rate correlations for single droplets, when applied to sprays, is suspect. In previous work (Burstein, Hammer, and Agosta) the use of these correlations gave calculated pressure histories within five percent of experimentally measured pressure histories. The liquid propellant in the droplets is completely mixed, uniform in temperature and composition and transport properties. The latter are functions of temperature. For the relaxation determination in the droplet evaporation rate, this assumption of thermal uniformity is not made. The gaseous film between the droplet surface and the flame sheath consists of combustion products and fuel vapor. Since the dissociation components and rates for the hydrazine are not known (Wagner, Gray) a simple mixture is assumed for these gases. The fuel vapor concentration manifests itself as a partial vapor pressure in this region. Adiabatic flame temperatures (allowing for heat transfer) are assumed at the outer boundary of the film. The stagnation temperature of the bulk gas is determined from heat transfer considerations and mixing with evaporation-decomposition products of the oxidant. The static pressure and temperature are determined from the fluid dynamics.

The approach is one-dimensional. Clearly, this assumption is not valid near the injector face. For any particular injector and combustion chamber design, a study must be made of the interdiffusion of chemical species and the role played by turbulent mixing. The results from this study will then be used either as perturbations in the steady flow equations, or as delineating geometrical regimes with different propellant-combustion gas compositions.

II. ANALYTIC FORMULATION

In this section the equation describing the processes contained in the combustion model are given.

A. Gas Dynamics.

From a volume of gas containing liquid droplets a volume element, $\delta\nu$, is selected containing one droplet. The droplet is evaporating and the ensuing vapors are burning. The gas and droplet velocities are $\overline{u}$ and $\overline{v}$, respectively, and the velocity of the droplet boundary with respect to the droplet center of mass is $\overline{w}$ (see Fig. 1). The conservation of mass is given by

$$\frac{\partial}{\partial t}\int_{\nu_g} \rho_g \delta\nu_g = \int_s \rho_g \overline{u}\cdot\overline{n}\,\delta s + \int_{s_\ell} \rho_\ell \overline{w}\cdot\overline{n}\,\delta s_\ell \tag{1}$$

where ρ_g is the gas density, ρ_ℓ the liquid density and assumed constant, δs_ℓ a surface element on the droplet boundary, and δs a surface element on the boundary of the gas. By means of Gauss's theorem, Eq. (1) becomes

$$\int_\nu \frac{\partial\rho}{\partial t}\,\delta\nu + \int_\nu \nabla\cdot(\rho\overline{u})\delta\nu = \int_{\nu_\ell} (\nabla\cdot\rho_\ell\overline{w})\delta\nu_\ell\ . \tag{2}$$

It is assumed that no gaseous mass exists in the droplet volume element; thus,

$$\int_\nu \rho_g\delta\nu = \int_{\nu_g} \rho_g\delta\nu_g + \int_{\nu_\ell} \rho_g\delta\nu_\ell = \int_{\nu_g} \rho_g\delta\nu_g\ .$$

In the following symbols for the gas no subscript g is used.

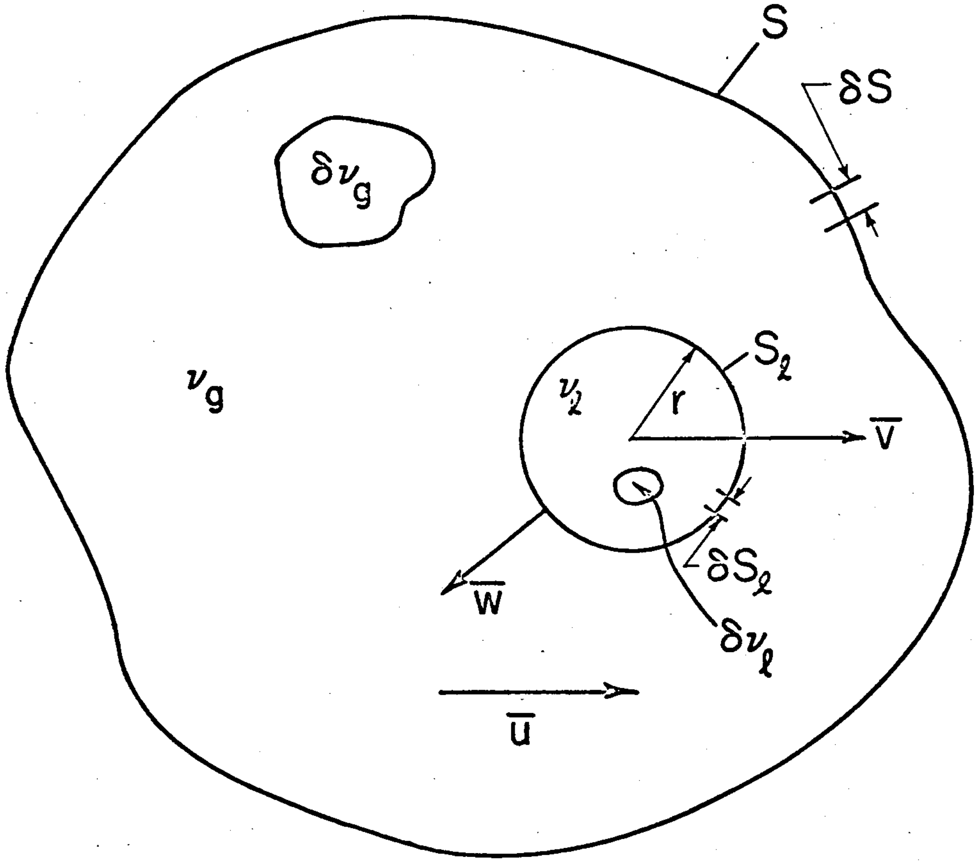

FIG. I THE DROPLET MODEL

For the one-dimensional case, Eq. (2) becomes

$$\frac{\partial}{\partial t}(\rho A) + \frac{\partial}{\partial x}(\rho u A) = \frac{\partial \varphi}{\partial x} \,, \tag{3}$$

where

$$(\nabla \cdot \rho_\ell \overline{w}) \equiv (\nabla \cdot \varphi) \tag{4}$$

It is noted that

$$\overline{n} \cdot \overline{w} = \frac{dr}{dt} \,, \tag{5}$$

where r is the droplet radius. Thus the right-hand side of Eq. (3) is determined from a coupled transport processes program describing droplet ballistics.

From Newton's second law the change of momentum of the droplet gas system is equated to the sum of forces acting on the system,

$$\frac{d}{dt}\int_\nu \rho \overline{u}\, \delta\nu + \frac{d}{dt}\int_{\nu_\ell} \rho_\ell \overline{v}\, \delta\nu_\ell = \int_s \overline{n}\, p\, \delta s \,, \tag{6}$$

where $\overline{v}$ is the droplet velocity and p the pressure assumed continuous throughout the volume element. Expanding the terms in Eq. (6) and again using Gauss's theorem gives

$$\int_\nu \rho \frac{d\overline{u}}{dt}\delta\nu + \int_\nu \overline{u}\frac{d(\rho\delta\nu)}{dt} + \int_{\nu_\ell} \rho_\ell \frac{d\overline{v}}{dt}\delta\nu_\ell + \int_{\nu_\ell} \overline{v}\frac{d(\rho_\ell \delta\nu_\ell)}{dt} = -\int_\nu \nabla p\, \delta\nu . \tag{7}$$

In the droplet-gas system the mass source for the gas is equal to the mass sink for the droplet; thus,

$$\int_{\nu_\ell} \frac{d}{dt}(\rho_\ell \delta\nu_\ell) = \int_\nu \frac{d}{dt}(\rho\delta\nu) = \int(\nabla \cdot \varphi)\delta x .$$

The droplet momentum varies due to a drag force acting on the drop, and this is defined by

$$\int_{\nu_\ell} \rho_\ell \delta\nu_\ell \frac{d\bar{v}}{dt} \equiv F . \qquad (8)$$

Combining Eqs. (3), (4), (7), and (8), the momentum equation becomes, for the one-dimensional case

$$\rho \frac{d(uA)}{dt} + (u-v)\frac{\partial\varphi}{\partial x} = - f - A\frac{\partial p}{\partial x} \qquad (9a)$$

where $F \equiv \int f\delta x$, or by expanding the terms

$$\frac{\partial(\rho u A)}{\partial t} + \frac{\partial(\rho u^2 A)}{\partial x} - v\frac{\partial\varphi}{\partial x} = - f - A\frac{\partial p}{\partial x} . \qquad (9b)$$

The energy equation is obtained from the First Law of Thermodynamics:

$$\int_\nu \frac{dQ}{dt}\delta\nu = \int_\nu \frac{dE^o}{dt}\delta\nu + \int_\nu \frac{dW}{dt}\delta\nu \qquad (10)$$

where Q is the heat transferred and is defined below, E^o the internal energy of the droplet-gas system, and W the work done by the gas. The change of the internal energy of the system is

$$\int_{\nu} \frac{dE^{o}}{dt}\,\delta\nu = \int_{\nu} \frac{d}{dt}(\rho\delta\nu e^{o}) + \int_{\nu_{\ell}} \frac{d}{dt}(\rho_{\ell}\delta\nu_{\ell} e^{o}_{\ell})\,. \tag{11}$$

Combining the above expression (11) with Eq. (2) gives

$$\int_{\nu} \frac{dE^{o}}{dt}\delta\nu = \int_{\nu} \rho\delta\nu\frac{de^{o}}{dt} + \int_{\nu_{\ell}} e^{o}(\nabla\cdot\rho_{\ell}\overline{w})\delta\nu_{\ell} + \int_{\nu_{\ell}} \rho_{\ell}\delta\nu_{\ell}\frac{d(e^{o}_{\ell\text{-}vap})}{dt} - \int_{\nu_{\ell}} e^{o}_{\ell}(\nabla\cdot\rho_{\ell}\overline{w})\delta\nu_{\ell}\,, \tag{12}$$

where the term $\int_{\nu_{\ell}} \rho_{\ell}\delta\nu_{\ell}\frac{d(e^{o}_{\ell\text{-}vap})}{dt}$ is the heat transferred to the droplet and goes toward heating and evaporating it. The heat transferred from the system can be written as

$$\int \frac{dQ}{dt}\,\delta\nu = \int \frac{d\overline{Q}}{dt}\,\delta\nu - \int_{\nu_{\ell}} \rho_{\ell}\delta\nu_{\ell}\frac{de^{o}_{\ell}}{dt} - \int_{\nu_{\ell}} \frac{dQ_{L}}{dt}\,\delta\nu\,, \tag{13}$$

where $\overline{Q}$ is the heat transferred from the gas and Q_L is the latent heat of vaporization of the droplet mass entering the gaseous system. The work done by the gas is

$$\int \frac{dW}{dt}\,\delta\nu = \int_{s} \overline{u}\cdot\overline{n}\,p\,ds + \int_{\nu_{\ell}} \rho_{\ell}\delta\nu_{\ell}\frac{d\overline{v}}{dt}\cdot\overline{v}\,. \tag{14}$$

It is assumed that the droplet mass does work on the gas during evaporation and moves at the gas velocity u. Thus, on expanding the surface integral and using Gauss's theorem and Eq. (2), the following expression results:

$$\int_s \overline{u}\cdot\overline{n}\,p\,ds+\int_{\nu_\ell}\rho_\ell\delta\nu_\ell\frac{d\overline{v}}{dt}\cdot\overline{v}=\int_\nu(\overline{u}\cdot\nabla p)\delta\nu+\int_\nu\frac{p}{\rho}\Big[\frac{\partial}{\partial\nu}\int\nabla\cdot(\rho_\ell\overline{w})\partial\nu_\ell-\frac{d\rho}{dt}\Big]\delta\nu$$

$$-\int_{\nu_\ell}\frac{p}{\rho_{vapor}}[\nabla\cdot(\rho_\ell\overline{w})]\,\delta\nu_\ell+\int_{\nu_\ell}\rho_\ell\delta\nu_\ell\frac{d\overline{v}}{dt}\cdot\overline{v}\,. \qquad (15)$$

Substituting expressions (9a), (12), (13), and (15) into Eq. (10), and assuming one-dimensional flow, gives

$$q=\rho A\frac{de^o}{dt}+\frac{\partial\varphi}{\partial x}[h^o-h_v^o]+uA\frac{\partial p}{\partial x}-\frac{p}{\rho}A\frac{dp}{dt}+fv \qquad (16a)$$

where

$$\int\frac{dQ}{dt}\delta\nu\equiv\int q\delta x \qquad (16b)$$

$$h^o=e^o+\frac{p}{\rho}\,, \qquad (16c)$$

and

$$h_v^o=e_\ell^o+Q_L+\frac{p}{\rho_{vapor}}\,. \qquad (16d)$$

An alternate form of Eq. (16a) which is more suitable is

$$q=\frac{\partial}{\partial t}(\rho Ae^o)+\frac{\partial}{\partial x}(\rho Auh^o)-h_v^o\frac{\partial\varphi}{\partial x}+fv\,. \qquad (17)$$

B. Fuel Droplet Ballistics.

Next, one considers the heat transfer effects on the fuel droplet. The drop is injected into the hot combustion gases at a fairly low temperature and hence an initial heating-up period is expected, provided that the injection temperature is lower than the wet-bulb temperature of the fuel.

Heat transfer processes are assumed to be predominantly by convection, and the net direction is from the combustion gases to the drop. Call this quantity of heat, q. Some of this energy actually heats the drop, (q_1), while part is used to vaporize the liquid, (q_v). Finally, some of the energy is used to heat the diffusing fuel vapor, (q_D). Therefore, the energy (q_{T_P}) that arrives at the surface of the j^{th} drop group is

$$q_{T_j} = q_1 + q_v = q - q_D \ . \qquad (18)$$

If K is the conductivity through the film, and A_1 the drop area, then

$$q_{T_j} = KA_1 \frac{dT}{dy} - wc_{p_1} (T - T_1) \ ; \qquad (19)$$

where T is the film temperature at position y, and y is the fraction of the film thickness; i.e., $y = r/\delta$, δ being the total film thickness, and r a radial position in the film. w is the rate of diffusing fuel vapor from the drop, at temperature T_1. If the specific heat of the fuel vapor c_{p_1} is constant throughout the film, then

$$\int_0^1 dy = \int_{T_1}^{T} \frac{KA_1}{q_T + wc_{p_1}(T - T_1)} \, dT \ . \qquad (20)$$

After integration and rearranging, it gives

$$q_{T_j} = \frac{KA_1 (T - T_1) z}{(e^z - 1)} = KA_1 (T - T_e) Z \ , \qquad (21)$$

where

$$z = \frac{wc_{p_1}}{KA_1} \quad \text{and} \quad Z = \frac{z}{e^z - 1} . \tag{22}$$

The term $KA_1(T-T_1)$ in Eq. (21) is the total heat transfer from the bulk gases to the drop. It is seen that the term $z/(e^z-1)$ is that correction factor applied to the heat transfer coefficient K, which was defined for the case without mass transfer. An experimental correlation of this form is used to obtain the heat transfer coefficient which is the Nusselt number for heat transfer.

$$q_v = hA_1(T-T_e)Z \tag{22a}$$

where

$$(Nu)_h = \frac{2hr_s}{Km} = 2 + 0.6\ Pr^{1/3} Re^{1/2} . \tag{22b}$$

It is noted that the coefficient of heat transfer h is substituted for the conductivity K. Here r_s is the droplet radius; h is the film coefficient; Km is the mean film conductivity; $Pr = \frac{c_p \mu}{K}$ is the Prandtl number, and $Re = \frac{2r|u-v|}{\mu/\rho}$ is the Reynolds number.

The temperature of the drop will vary in time since the sensible energy of the drop is related to the heat transfer. If the drop is followed in time, then

$$\frac{dT_1}{dt} = \frac{q_1}{c_1 m_1} \tag{23}$$

where c_1 is the specific heat of the liquid and m_1 is the instantaneous mass of the drop and t is the time. An energy balance around the drop yields a relation for q_1 in terms of λ, the latent heat of evaporation.

$$q_1 = q_{T_j} - w\lambda \tag{24}$$

Since the radius of the drop, r_s, the diffusion rate, w, and the velocity of the drop, v, are necessary pieces of information for the computation of the heat transfer through the film at any instant, a knowledge of the amount of mass transferred by the drop to the bulk gas must be known. On a semi-empirical basis, the diffusion rate is usually given as

$$w = K_g A_1 p_1 \alpha \tag{25}$$

where K_g is the coefficient of the mass transfer, and can be determined from the following equation:

$$(\mathrm{Nu})_{K_g} = \frac{2K_g r\overline{T}}{D_v M_g / R} = 2 + 0.6 \mathrm{Sc}^{1/3} \mathrm{Re}^{1/2} \tag{26}$$

Equation (26) is based on pure film diffusion while thermal diffusion (Dufour effect) is neglected. The following notation has been used in the last two equations: M_g is the molecular weight of the diffusing vapor; $S_c = \frac{\mu}{D_v \rho}$ is the Schmidt number; p_1 is the vapor pressure at the liquid drop temperature; and α is a correction factor to account for the uni-directional diffusion process rather than just considering the equimolar diffusion coefficient, K_g, which is computed from Eq. (26). α is given as

$$\alpha = \frac{p}{p_1} \, \mathrm{Ln} \frac{p}{p - p_1} \tag{27}$$

The values of D_v, the diffusion coefficient, were obtained by using the techniques recommended by Hirschfelder, Curtiss and Bird, "Molecular Theory of Gases and Liquids," John Wiley. If one defines a reduced temperature T_R as $\overline{T}/(T_{ca}T_{cb})^{\frac{1}{2}}$, where $\overline{T} = (T_1+T)^{\frac{1}{2}}$ and in addition, if, for a two-component system the critical temperatures, pressures, and molecular weight are known, then the diffusivity is

$$D_v = \frac{(p_{ca}p_{cb})^{1/3}(T_{ca}T_{cb})^{5/12}}{\left(\frac{2M_aM_b}{M_a+M_b}\right)^{\frac{1}{2}}} \frac{a}{p} T_R^b \tag{28}$$

Here, p_{ca}, T_{ca}, and M_a are the critical pressure, temperature, and molecular weight of the fuel; p_{cb}, T_{cb}, and M_b are the average critical pressure, temperature, and molecular weight of the products of combustion.

It is seen then that to evaluate mass transfer, a knowledge of the heat transfer, radius, and velocity of the droplet at any instant is required. Consider the change in the radius of the drop with time, which can be computed from the continuity equation for the liquid drop,

$$\frac{d\rho_1\nu_1}{dt} = \left[\frac{\partial\rho_1\nu_1}{\partial t} + V_e \frac{\partial\rho_1\nu_1}{\partial x}\right] = -w. \tag{29}$$

Here, $\nu_1 = 4/3\,\pi r^3$ is the volume of the liquid drop. The mass that is combusting per drop is $(w\Delta t)$, and the total mass that has combusted is

$$W = \sum_j (w\Delta t)N_j \tag{30}$$

where N_j is the number of drops per second flowing in the combustion process for the j^{th} class. $\varphi = \int_0^x W dx$ is the total mass combusted (per unit time) up to a position x in the combustion chamber. This position is measured from the injector face.

Introducing the radius in terms of the volume of the drop, the variation of r with respect to time may be expressed in terms of the evaporation or diffusion rate, w. w is obtained from mass transfer considerations and the temperature variation dT/dt, the latter being obtained from heat transfer considerations.

$$\frac{dr}{dt} = - \frac{w}{A_1 \rho_1} - \frac{r}{3\rho_1} \left(\frac{d\rho_1}{dT_1}\right) \frac{dT_1}{dt} \tag{31}$$

Since $d\rho_1 / dT_1 < 0$, the drop radius will first increase in time due to the heating up of the drop and then will decrease as the first term on the right-hand side of Eq. (31) predominates.

The velocity of the droplet at any instant during the evaporation process is necessary to the calculation of the correlations of heat and mass transfer. Aerodynamic drag forces will either slow the droplets down or speed them up, depending on the sign of the relative magnitude of the gas velocity compared to the droplet velocity, v.

The force exerted on a single spherical drop of mass m_1, is $m \frac{dv}{dt} = \frac{4}{3} \pi r^3 \rho_1 \frac{dv}{dt} = - F$. From aerodynamic theory, the drag force exerted by a moving fluid on an immersed body is $C_D A \rho \frac{(u-v)^2}{2}$. C_D is the coefficient of drag for a given shape, and is a function of the Reynolds number. A is the cross-sectional area of the body, i. e., (πr^2), and ρ is the density of the fluid. By equating the two forces, one obtains an equation expressing the dynamic behavior of the droplets

$$\frac{dv}{dt} = -\frac{3}{8} C_D \frac{\rho}{\rho_1} \frac{(u-v)|u-v|}{r} . \tag{32}$$

Here C_D is the instantaneous drag coefficient for the liquid droplets and is given as

$$C_D = \frac{27}{Re^{0.84}} \tag{33}$$

when $6 < Re < 400$. This condition is readily met in the present computations, as the mean value of $Re \approx 150$.

The drop velocity lags behind the gas velocity over most of the combustion chamber, except near the injector face, where the gas velocity is low. In the regions where the drop velocity lags behind the gas velocity, it was felt that the drop might shatter due to large shear forces. In addition, drop breakup can occur if the temperature of the fluid became supercritical. Liquid temperatures could not physically go to the critical point without reduction of the surface tension, i.e., to the point where droplet stability is impaired. Therefore, provision was made for the droplet to be replaced by an arbitrary number of smaller drops of equal mass whenever a stability criterion was exceeded. The Weber number is the stability criterion used, since it is a ratio of the aerodynamic pressures over the surface of the droplet compared to the surface tension acting through the curvature, i.e.,

$$We = \frac{2r_s(u-v)^2\rho}{\sigma_1} \tag{34}$$

The drop size distribution in the fuel spray will be treated in a similar manner to that of the oxidant, which is presented below.

C. Oxidant Droplet Ballistics.

The evaporation analysis for the oxidant is given below. On the basis of kinetic theory, it can be shown that when a uniform gas with no mass motion is bounded by a surface, the mass of molecules striking a unit area of that surface can be given by

$$G = (1/4)m\nu\overline{v} \tag{35}$$

where G is the mass of the ensemble of molecules, M the molecular mass, ν the molecule population density, and $\overline{v}$ the average velocity. The ideal equation of state

$$p = \rho R_o T/M \tag{36}$$

and

$$\rho = \nu m \tag{37}$$

gives

$$G = p\sqrt{Mg/2\pi R_o T} \tag{38}$$

where p is the gas pressure, ρ the gas density, R_o the universal gas constant, M the molecular weight, and T the gas temperature.

The assumptions used in the evaporation analysis are given below:

(1) The accommodation coefficient is initially unity. This assumption will apply to any existing undissociated oxidant. It is recognized that some of the oxidant dissociated components can dissolve into the droplet; however, for the droplet temperatures envisaged, this amount will be very small and thus negligible. Theoretically, for the first few

intervals for thermodynamic conformity, it is expedient to use this assumption, even though from a practical viewpoint its effect can be negligible. After the first interval the accommodation coefficient will adjust according to the gas-vapor composition on the droplet surface.

(2) The rocket engine chamber wall temperature is constant during the propellant evaporation.

(3) A steady state calculation is made employing oxidant droplet ballistics based on the propellant distribution given below and requiring about 95 percent of the propellants to evaporate. The results of these calculations give the propellant drop sizes. A logarithmiconormal drop size distribution is chosen

$$\frac{dR}{dr} = \frac{100}{\sqrt{2\pi}\, r \ln \sigma} \exp\left[-\frac{1}{2}\left(\frac{\ln(r/\overline{r})}{\ln \sigma}\right)^2 \right. \qquad (39)$$

where R is the percent mass in drops smaller than given radius r, r the drop radius, $\overline{r}$ the mass median drop radius and σ the geometric standard deviation. The spray is divided into several different groups of drop sizes so that drop histories can be calculated. The sizes are obtained from the logarithmic probability distribution function as thos average radii for which R, the percent mass in drops smaller than the radius, is, say, 30, 70 and 95 percent. Thus the radii for R equal to 30, 70, and 95 percent are obtained for a given σ and $\overline{r}$. Then the arithmetic mean radii are selected to represent each group which have been chosen so that, corresponding to the above quantities, 30 percent of the mass exists in the first group, 40 percent in the second group, and 30 percent in the last group. The mass conservation law is then employed to determine the number of drops in each of the drop size groups. Thus, from the distribution function for given values of σ and $\overline{r}$, the drop sizes are obtained.

The number of drops N_i in each group is determined by

$$N_i = W_i/(4/3)\pi r^3 \rho \tag{40}$$

where W_i is the mass of drops in each group. The total mass of drops in the three groups, i. e., the droplet ensemble is

$$W_j = \sum_{i=1}^{3} W_{ji} \tag{41}$$

which is the mass of liquid propellant injected during the j^{th} interval of time. The number of drops in each group is accordinly determined.

The total number of drops during the j^{th} interval is

$$N_j = \sum_{i=1}^{3} N_{ji} = K_1 W_j/\rho_\ell \tag{42}$$

In addition, the drop surface area before evaporation occurs is

$$A_{ji} = 4\pi r_i^2 N_i = 4\pi r_i^2 (N_i/N_j)N_j \tag{43}$$

$$A_j = \sum_{i=1}^{3} A_{ji} = K_2 N_j \tag{44}$$

(4) Time intervals are taken short enough so that all properties remain essentially constant during that interval.

(5) The molecular weight of the "vapor" is determined from the molecular weight of the dissociation components of the oxidant. Since

the vapor pressure is less than the bulk gas pressure, combustion gas products are also colliding in the oxidant droplet. A thermochemical calculation for equilibrium conditions must thus be made.

(6) The gas evaporates at the same temperature as the liquid drops from which it is evolved.

(7) The oxidant jet breakup is instantaneous and complete at time zero.

(8) The solution proceeds from known initial conditions to calculate new values of properties at the end of the first time interval. The new values are assumed as initial conditions for the second time interval, and so on to completion.

From Eq. (38) the amount of evaporation occurring in a finite time interval is given by

$$G_{evap} = \left\{ .0578 [P_v(T_d) - P_g(T_g)] \sqrt{M/T_d} \right\} A_d \Delta t. \tag{45}$$

Expressing the drop area as a function of radii total injected weight flow and density, the total evaporation occurring during the Nth time interval is given by

$$G_{evap} = \sum_{i=1}^{3} \sum_{j=1}^{N} G_{ij} \tag{46}$$

and

$$G_{ij} = C_i [P_v(T_d)_{ijN-1} - P_g(T_g)_{N-1}] \frac{r^2_{ijN-1} \sqrt{M} W_j \Delta t_N}{\rho_\ell \sqrt{(T_d)_{ijN-1}}}, \tag{47}$$

where $P_v(T_d)_{ijN-1}$ is the vapor pressure measured at the temperature of the i^{th} size drop of the j^{th} group at the end of the N-1 time interval.

The above expression (47) yields the evaporation during the N^{th} time interval for each of the various sized drops, in each of the j groups ($1 \leq j \leq N$). j can start at a number higher than 1, since it is possible that the initial drop ensembles become completely evaporated as time increases. Pressure, temperature and radii are evaluated at the end of the previous time interval, (N-1). Whenever j=N, drop radii and temperature are given by the initial conditions, since a slug of mass has just been injected into the chamber. The heat transfer to the oxidant droplet is treated in a similar manner as that to the fuel droplet. A question arises as to the thickeness of the "film" around the droplet, and the temperature of the outer edge of the "film." This matter was discussed above and requires further study.

D. Thermochemistry.

There now remains the chemistry to be determined. Since the oxidant evaporation rate is greater than that of the fuel, then combustion occurs at various O/F ratios. This condition must be reflected in the chemistry of combustion. It is envisaged at this time to consider, at any spacial interval in the chamber, a mixture of oxidant rich bulk gases, plus an increment of fuel and oxidant as determined from their respective ballistics. A mixture of these "three" components will occur, their properties being determined by solving the thermodynamic chemical equilibrium equations for the atomic constituents. It is seen that combustion occurs at oxidant rich conditions, the design O/F ratio being approached toward the completion of combustion, i. e., the disappearance of the fuel droplets. Thus the equilibrium equations should reflect those components which occur in an oxidant rich reaction. This is fortuitous in that at the present time the concentrations of the dissociation components of hydrazine are not well-known. In addition, fuel lean mixtures tend to yield simple combustion products and excess oxidant also tends to decompose into its elements.

Recent experiences have shown that use of a subroutine containing the equilibrium chemical calculation requires a prohibitive amount of computer time. It is suggested that a table of enthalpy-pressure-combustion constituents be compiled and used in the thermochemical subroutine. These should be available for various O/F ratios. In order to conserve computer time, it would be more efficient if a table were set up containing the functional values of the enthalpy and the pressure. I stress this point because an inordinate amount of computer time (2 hours of IBM 7094) was consumed in iterations in the gas dynamic-thermochemical subroutines.

III. DESCRIPTION OF COMPUTATION WORK

The overall algorithm for the calculation is shown on Figure 2. A first guess is made on the oxidizer droplet evaporation profile and on the gas properties. Based on these guesses, a fuel droplet evaporation profiles is calculated. From this profile and from the assumed oxidizer evaporation profile, the gas properties are recalculated. If these gas properties do not match the assumed ones, the fuel droplet evaporation profile is recalculated using the new gas properties. The check and

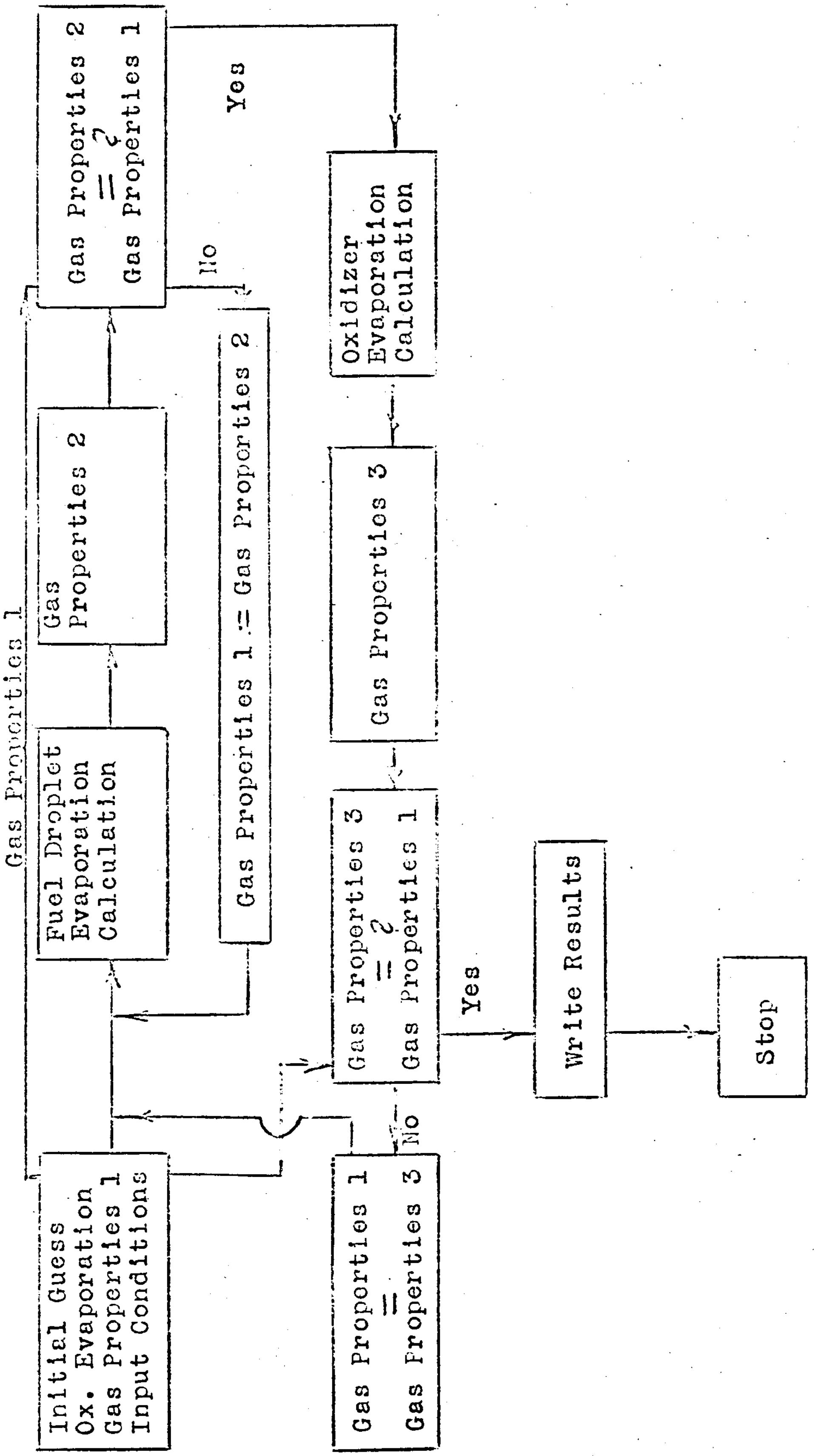

Figure 2. Algorithm For The Overall Calculation 1

recalculation is repeated until the gas properties no longer change from one calculation to the next. This final set of gas properties is used to recalculate the oxidizer droplet evaporation profile. This new oxidizer evaporation profile replaces the originally assumed one, and the gas properties are again recalculated. If the new gas properties match the previously calculated ones, the calculation is finished. If they do not match, the original oxidizer evaporation profile is replaced by the latest calculated version, the gas properties are replaced by the newly calculated ones, and the calculation starts all over again from the beginning.

It may be noted that, in this algorithm, the fuel evaporation profile is calculated many more times than is the oxidizer evaporation profile. The reason for this is that there is a much greater likelihood of guessing the oxidizer evaporation profile accurately at the start than the fuel evaporation profile. Thus, this algorithm would tend to minimize the amount of computer time required for the overall computation, since it would minimize the number of times the gas properties are recalculated. The gas property calculation is the most time consuming part of the program.

In the various parts of the computer program the differential equations representing heat, mass, and momentum balances are written in difference form. The rocket chamber is divided into a number of small increments. The difference equations, written for an increment, are used to generate properties at the end of each increment when the properties at the beginning of the step are given. In this way, we start at the injector face and proceed downstream until we reach the nozzle and match the boundary condition prescribed at the sonic point.

This solution logic is quite preliminary and requires a great deal of modification. It is discussed here because as a first approach, it has worked. It suffers from requiring an excessive amount of computer time. This defect will be overcome.

Subsequent to this computation, a primitive model was constructed. It is shown in Figure 3. It is based on an assumed oxidizer evaporation rate (step function) while using a constant O/F ratio throughout the chamber. This implies that the chemistry is known for all times. Solutions can be obtained on the order of .1 hours.

The assumption concerning the evaporation of the oxidizer may be valid when the oxidizer has characteristics which distinguish it readily from the fuel, i. e. , the rate controlling assumption is known to be valid. In some cases, neither fuel nor oxidizer is rate controlling. Hence, it is not a reasonable procedure to carry out a complete calculation involving k iterates for the fuel based on an assumed oxidizer rate.

It is proposed to carry out the computation in a parallel fashion rather than in the serial procedure shown in Figures 2 and 3. The effect of the variable O/F ratio will be taken into account through table hookups for specific heats, enthalpies and molecular weights at a constant pressure, rather than a calculation of the minimization of Gibbs Free energy for (T_jp) variable. It is felt that the variation of pressure will be small in the chamber, especially in and near the injector face.

The parallel procedure will involve a complete solution (with the above table hookups) at each step (with and without droplet breakup). This type of calculation will do away with the major amount of computing time

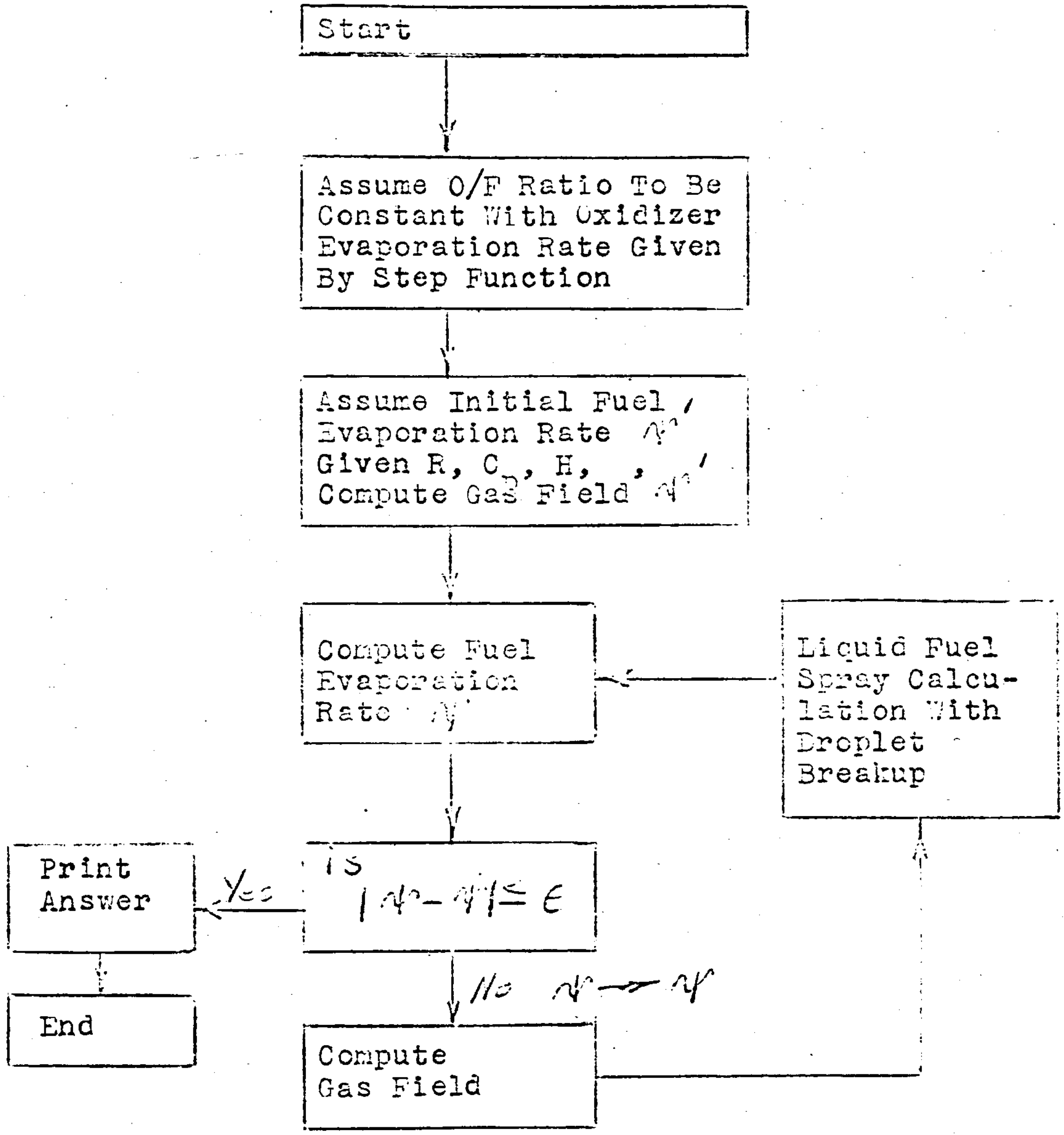

Figure 3. Algorithm For The Overall Calculation

spent calculating complete histories based on initially poor data.

Once we know a good approximation to the solution, chemistry can be switched as a final computation pass is made for all the p drop groups in the chamber (see Figure 4).

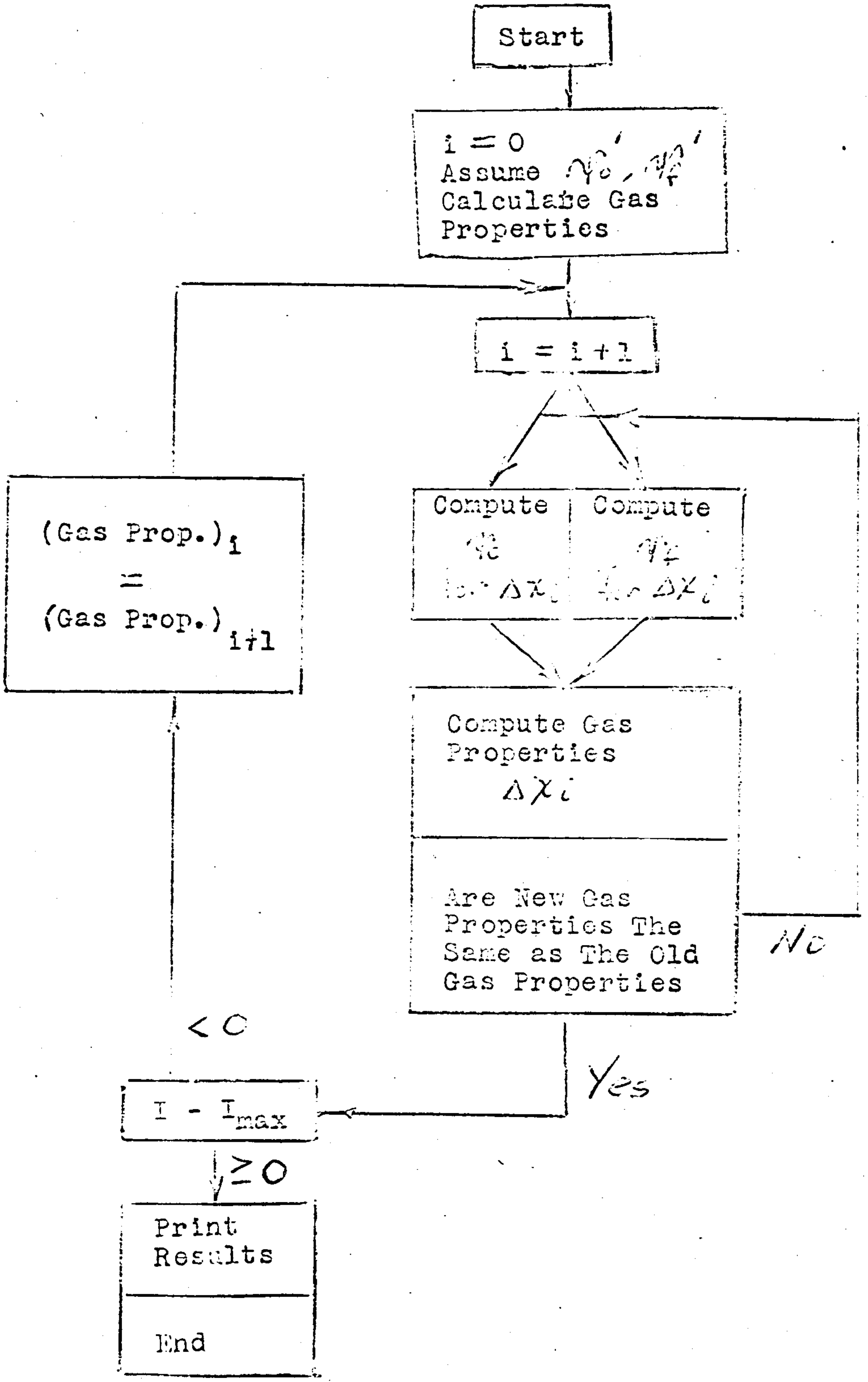

Figure 4. Algorithm For The Overall Calculation 111